

See discussions, stats, and author profiles for this publication at: <https://www.researchgate.net/publication/231706567>

# Hydrogen Bonded Supramolecular Elastomers: Correlating Hydrogen Bonding Strength with Morphology and Rheology

ARTICLE in *MACROMOLECULES* · FEBRUARY 2010

Impact Factor: 5.8 · DOI: 10.1021/ma9027646

---

CITATIONS

40

---

READS

56

7 AUTHORS, INCLUDING:



**Daniel Hermida Merino**

European Synchrotron Radiation Facility

38 PUBLICATIONS 492 CITATIONS

SEE PROFILE



**Barnaby W Greenland**

University of Reading

42 PUBLICATIONS 1,044 CITATIONS

SEE PROFILE



**Ian W Hamley**

University of Reading

404 PUBLICATIONS 11,809 CITATIONS

SEE PROFILE

## Hydrogen Bonded Supramolecular Elastomers: Correlating Hydrogen Bonding Strength with Morphology and Rheology

Philip J. Woodward,<sup>†</sup> Daniel Hermida Merino,<sup>†</sup> Barnaby W. Greenland,<sup>†</sup> Ian W. Hamley,<sup>†</sup> Zoe Light,<sup>†</sup> Andrew T. Slark,<sup>‡</sup> and Wayne Hayes<sup>\*†</sup>

<sup>†</sup>Department of Chemistry, University of Reading, Whiteknights, Reading, RG6 6AD United Kingdom, and

<sup>‡</sup>Henkel U.K. Limited, Wexham Road, Slough, SL2 5DS United Kingdom

Received December 15, 2009; Revised Manuscript Received January 22, 2010

**ABSTRACT:** A series of six low-molecular-weight elastomers with hydrogen bonding end groups have been designed, synthesized, and studied. The poly(urethane)-based elastomers all contained essentially the same hard block content (ca. 11%) and differ only in the nature of their end groups. Solution-state <sup>1</sup>H NMR spectroscopic analysis of model compounds featuring the end groups demonstrates that they all exhibit very low binding constants in the range of 1.4 to 45.0 M<sup>-1</sup> in CDCl<sub>3</sub>, yet the corresponding elastomers each possess a markedly different nanoscale morphology and rheology in the bulk. We are able to correlate small variations of the binding constant of the end groups with dramatic changes in the bulk properties of the elastomers. These results provide important insight into the way in which weak noncovalent interactions can be utilized to afford a range of self-assembled polyurethane-based materials that feature different morphologies.

### Introduction

Supramolecular polymer chemistry has become a major field of research in recent years.<sup>1</sup> In typical, supramolecular polymers consist of relatively low-molecular-weight species that are able to assemble spontaneously into higher ordered structures through designed motifs that can form reversible noncovalent bonds.<sup>2</sup> Supramolecular materials utilizing hydrogen bonding interactions have received<sup>3,4</sup> the most widespread attention, but in principle, any noncovalent bond-forming process could be employed, as demonstrated by the synthesis of materials harnessing the dynamic nature of metal–ligand complexation<sup>5</sup> and  $\pi$ – $\pi$  stacking<sup>6</sup> interactions to form supramolecular materials.

As with conventional, covalently bonded polymers, the macroscopic properties of supramolecular polymers (such as viscosity and tensile strength) are intimately related to the degree of polymerization (DP). For supramolecular polymers in dilute solution, the relationship between monomer concentration ([M]) and DP can be approximated<sup>7</sup> to be proportional to ( $K_a[M]$ )<sup>0.5</sup>, where  $K_a$  is the association constant of the monomers. In these systems,  $K_a$  can be altered by the application of an external stimulus that directly affects the physical properties of the polymer. Subsequent removal of the stimulus allows the supramolecular bonds between the monomers to reform, thus restoring the original mechanical properties of the material. This characteristic affords supramolecular systems with reversibly switchable physical properties, a feature that cannot be achieved easily through conventional covalent polymer synthesis. As a consequence of the relationship between DP and  $K_a$ , early studies in this field focused on increasing the binding constant between the monomeric components of the supramolecular polymer. This resulted in the production of materials with solution-state properties analogous to those of conventional high-molecular-weight covalently bonded polymers. As a result, carefully designed,

highly preorganized hydrogen bonding motifs that exhibit high binding constants ( $< 10^6$  M<sup>-1</sup>) were reported by the groups of Meijer and Sijbesma<sup>8</sup> and Zimmerman.<sup>9</sup> Bulk supramolecular polymers that are assembled from monomers that exhibit high binding constants require significant energy to disrupt the supramolecular assembly. Therefore, disassembly of the supramolecular complexes to give dramatic changes in viscosity requires high temperatures (for example,<sup>10</sup> the storage modulus ( $G'$ ) of a supramolecular complex composed of tetraethylene glycol bis(4-benzoic acid) and 2,2',6,6'-tetrakis[(4-pyridyl)methylene] iminophenoxylbiphenyl] only decreased by an order of magnitude when the temperature was increased from 150 to 190 °C ( $4.5 \times 10^6$  to  $2 \times 10^5$  Pa).

Whereas the relationship among DP,  $K_a$ , and the physical characteristics of supramolecular polymers in dilute solution is well understood, the same rational cannot be applied directly to the prediction of bulk properties of the materials. In the solid state, polymer morphology and crystallinity play equally important roles in the final properties of the material. Early reports of these relationships include studies by Lillya et al., who found<sup>11</sup> that the addition of simple benzoic acid residues to low-molecular-weight poly(tetrahydrofuran) (PTHF) ( $M_n \approx 2000$  Da) transformed the waxy parent polymer to an elastomeric solid. The strength of the material is derived from crystallization of the end groups into hard microdomains<sup>12</sup> that afford the polymer a 3D network structure. Rheological analysis demonstrated that the storage modulus for the self-assembled material decreased from  $10^6$  to  $\sim 0$  Pa between 50 and 70 °C. Dramatic changes in viscosity such as this over readily accessible temperatures represent a genuine advantage for large-scale polymer synthesis and processing. Because of this report, stable supramolecular assemblies generated by phase segregation driven by crystallinity and hydrogen bonding have been studied by several groups.<sup>13–15</sup> Notably, Rowan et al. have demonstrated the ability to harness the cooperative power of multiple weak hydrogen bonding units ( $\sim 5$  M<sup>-1</sup>) from the addition of adenine derivatives to PTHF ( $M_n = 1400$  g mol<sup>-1</sup>).<sup>16</sup> This procedure transformed soft waxy

\*Corresponding author. Fax: (+44) 118-378-6331. E-mail: w.c.hayes@reading.ac.uk.

PTHF into a highly thermally sensitive material that was mechanically stable under ambient operating temperatures. ( $G'$  is ca.  $10^6$  at 120 °C.)

We have recently reported the synthesis of a series of low-molecular-weight (< 650 Da) bisurethane derivatives via a simple one-pot procedure from inexpensive and readily available starting materials.<sup>17</sup> Extensive  $^1\text{H}$  NMR, IR spectroscopic, and viscometric analysis demonstrated that these bisurethane species assembled into extended hydrogen-bonded networks both in solution and in bulk. Rheological analysis in the bulk revealed that these bisurethanes behaved in an analogous fashion to high-molecular-weight polyurethanes ( $M_w \approx 50\,000\text{ g mol}^{-1}$ ) despite their monomeric nature and low association constants ( $> 15\text{ M}^{-1}$ ). Furthermore, we have also demonstrated<sup>18</sup> that this bisurethane hydrogen bonding motif could be readily introduced into isocyanate terminated prepolymers. The addition of the end group to the prepolymer was found to have a dramatic effect on the physical properties of the bulk material, transforming the viscous prepolymers into elastomers that exhibited highly temperature-dependent rheological characteristics. These elastomers were synthesized through a simple procedure that involved the addition of either an alcohol or amine derivative to a prepolymer, followed by isolation via precipitation. This methodology permits the rapid production of a series of structurally related materials enabling the influence of atomic level changes to either the hydrogen bonding “hard” segments or the polymer “soft” segments to be investigated in a systematic fashion. Herein we report the results of a structure–property investigation of series of self-assembling polyurethanes by correlating changes in hydrogen bonding ability on the nanostructure and mechanical properties of the bulk elastomers.

## General Experimental Section

**Materials.** Poly(ethylene-*co*-butylene) diol ( $M_n = 3500$ ,  $M_w/M_n = 1.08$ ) was supplied by Henkel U.K. Limited. Reagents were purchased from Acros Chimica, Aldrich Chemical, and Alfa Aesar and were used without further purification. Tetrahydrofuran (THF) was distilled from benzophenone and sodium.

**Characterization.**  $^1\text{H}$  NMR spectroscopy was performed on a Bruker AMX400 (400 MHz) spectrometer or a Bruker AC250 (250 MHz) spectrometer (using the deuterated solvent as lock).  $^{13}\text{C}$  NMR spectroscopy was performed on Bruker AMX400 (100 MHz) spectrometer or a Bruker AC 250 apparatus operating at 62.5 MHz. Infrared spectroscopy was performed using either a Perkin-Elmer 1720-X spectrometer or a Bruker Equinox 55 FT-IR microspectrometer fitted with an MCT D316 IR scope detector in transmission mode. The samples were analyzed as either neat films or in solution between two potassium bromide or sodium chloride disks. Gel permeation chromatography (GPC) was performed by Smithers RAPRA U.K. using a Viscotec TDA model 301 equipped with a PLgel guard column and two mixed-bed-D (30 CM, 5  $\mu\text{M}$ ) columns. Detection was achieved using a refractive index detector with differential pressure and light scattering. The samples were analyzed at 30 °C using THF as the eluent at a flow rate of 1 mL/min. The instrument was calibrated using low polydispersity polystyrene standards. Glass-transition temperatures ( $T_g$ ) were determined using a TA Instruments DSC 2920 differential scanning calorimeter. DSC was performed scanning from  $-80$  to  $150$  °C (at a rate of 3 K/min modulated). Rheological analysis was performed on a TA Instruments AR2000 rheometer at a constant frequency of 10 Hz.

SAXS experiments were performed on station 2.1 at the Synchrotron Radiation Source, Daresbury Laboratory, U.K. and station A-2 of HASYLAB at Deutsches Elektronen-Synchrotron (DESY) in Hamburg, Germany. A 2D RAPID area detector was used on station 2.1 at Daresbury to acquire SAXS patterns. WAXS data were obtained at station A-2 DESY using

a linear detector. Because orientation was not observed in the SAXS patterns, data were reduced to the 1D form using software BSL with appropriate background subtraction. The wavenumber  $q = 4\pi \sin\theta/\lambda$  (scattering angle  $2\theta$ , wavelength  $\lambda = 1.5$  or  $1.4$  Å) scale was calibrated using wet collagen (rat tail tendon).

Full synthetic procedures and characterization for the model compounds can be found in the Supporting Information. Binding constants were determined by a dilution titration followed by  $^1\text{H}$  NMR spectroscopic analysis. (See the Supporting Information.) These data were analyzed by “Dynofit 4” to generate the binding constant and confidence interval using the Michaelis–Menten equation

$$\delta[T] = \delta_{\text{max}} - \frac{\Delta\delta_{\text{max}} \times K_a \times [T]}{1 + K_a \times [T]}$$

**Synthesis of Isocyanate Terminated Prepolymer 14.** Poly(ethylene-*co*-butylene) diol **13** (250.0 g, 0.071 mol) was heated at 120 °C under vacuum for 1 h before MDI (35.7 g, 0.143 mol) was added to the stirred polymer under a nitrogen atmosphere. After 60 min of heating, a vacuum was applied for 30 min before the heat was removed, and the system flushed with nitrogen to generate prepolymer **14**, which was then stored at  $-18$  °C and used as required.

Polymers **16**, **18**, and **19** were prepared according to the general procedure described for **15**. (See the Supporting Information.)

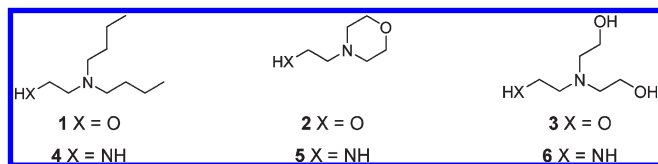
**4-((4'-Carbamic Acid 2-[bis-Butyl-amino]-ethyl Ester) Benzyl)-phenyl-amino-carbonyl-Terminated Poly(ethylene-*co*-butylene) Diol 15.** To a stirred solution of prepolymer **14** (4.34 g, 0.362 mmol) in dry THF (50 mL) under a nitrogen atmosphere was added 2-hydroxyethyl-*N,N*-bis-butylamine (0.45 mL, 2.2 mmol), and the mixture was heated under reflux for 18 h. The material produced was purified by repeated precipitation from methanol at  $-78$  °C to furnish the desired polymer **15** as a clear light-brown tacky wax material (3.85 g, 71%). IR ( $\text{CDCl}_3$ , KBr,  $\nu_{\text{max}}/\text{cm}^{-1}$ ): 2904, 2855, 1728, 1613, 1595, 1523, 1461, 1413, 1379, 1310, 1216, 1064.  $^1\text{H}$  NMR (400 MHz,  $\text{CDCl}_3$ ,  $\delta$ ): 0.81–0.84 (m), 0.88–0.92 (m), 1.03–1.26 (m), 1.60–1.70 (m), 2.46–2.50 (t,  $J = 7.5$  Hz), 2.71–2.74 (t,  $J = 6.0$  Hz), 3.88 (s), 4.12–4.22 (m), 7.09–7.20 (m), 7.26–7.29 (m).  $^{13}\text{C}$  NMR (100 MHz,  $\text{CDCl}_3$ ,  $\delta$ ): 10.6–11.1, 14.3, 20.9, 26.1–27.0, 29.6, 30.0–31.2, 33.5–33.8, 38.1–39.1, 40.8, 52.9, 54.7, 63.5, 63.9, 119.1, 129.6, 136.3, 136.5, 154.0. GPC (THF):  $M_w$  27 000,  $M_n$  15 200.

Polymer **20** was prepared according to the general procedure described for **17**. (See the Supporting Information.)

**4-((4'-Carbamic Acid 2-[bis-(2-Hydroxyethyl)-amino]-ethyl Ester) Benzyl)-phenyl-amino-carbonyl-Terminated Poly(ethylene-*co*-butylene) Diol 17.** To a stirred solution of triethanolamine (0.38 g, 2.6 mmol) in dry THF (10 mL) under reflux was added dropwise a solution of prepolymer **14** (5.00 g, 0.417 mmol) in dry THF (125 mL). After 1 h, the reaction was cooled to room temperature, and the product isolated by repeated precipitation from methanol at  $-78$  °C to furnish **17** as a clear colorless elastomer (3.36 g, 62%). IR ( $\text{CDCl}_3$ , KBr,  $\nu_{\text{max}}/\text{cm}^{-1}$ ): 3436, 3154, 2961, 2926, 2854, 1793, 1729, 1595, 1522, 1463, 1413, 1380.  $^1\text{H}$  NMR (400 MHz,  $\text{CDCl}_3$ ,  $\delta$ ): 0.80–0.85 (m), 1.07–1.26 (m), 1.60–1.70 (m), 2.71–2.75 (t,  $J = 5.0$  Hz), 2.81–2.85 (t,  $J = 5.5$  Hz), 3.60–3.63 (t,  $J = 5.0$  Hz), 3.88 (s), 4.14–4.25 (m), 7.04–7.08 (m), 7.26–7.30 (m).  $^{13}\text{C}$  NMR (100 MHz,  $\text{CDCl}_3$ ,  $\delta$ ): 10.6–10.9, 25.9–26.8, 30.0–31.2, 33.5–33.8, 38.1–39.1, 40.5, 54.3, 56.9, 59.6, 63.2, 63.9, 118.8, 129.4, 136.0, 136.2, 153.9. GPC (THF):  $M_w$  35 100,  $M_n$  17 000.

## Results and Discussion

The initial focus of this investigation was the design of supramolecular urethane-based polymers that feature end groups that possess varying degrees of hydrogen bonding capability to

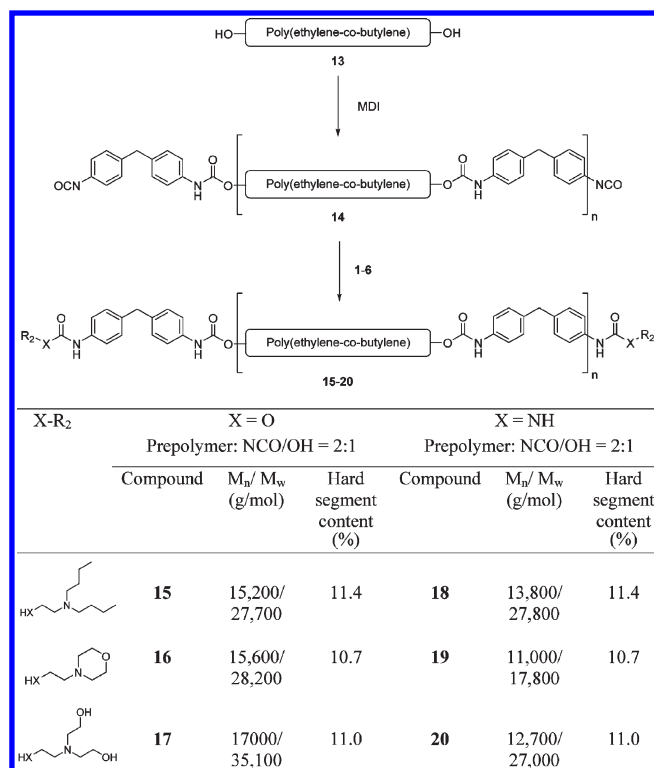
**Figure 1.** Structures of end groups 1–6.**Table 1.** Structures and Binding Constants (CDCl<sub>3</sub>, 25 °C) for the Model Compounds 7–12

Compound	$K_B/M^{-1}$		$R_1$
	X = O	X = NH	
	<b>7</b> 1.4 ± 0.4	<b>10</b> 6.9 ± 1.7	<b>7</b> = undecane <b>10</b> = 2-ethylhexane
	<b>8</b> 1.5 ± 0.3	<b>11</b> 9.7 ± 4.5	<b>8</b> = undecane <b>11</b> = 2-ethylhexane
	<b>9</b> 15 <sup>17</sup>	<b>12</b> 45 ± 11	<b>9</b> = decane <b>12</b> = 2-ethylhexane

realize “tunable” materials. The end groups were selected in line with our previous investigations<sup>17,18</sup> to deliver materials that possessed a noncrystalline, yet interpenetrating phase-separated morphology. These design criteria are important because the introduction of physical, crystalline cross-links into noncovalently bonded polymeric materials has previously been shown to have a dramatic impact on the physical properties of the materials, over and above the hydrogen bonding interactions that we aimed to study.<sup>11,16</sup> In addition, recent work by Sibjesma et al. has demonstrated<sup>19</sup> that telechelic supramolecular polymers that assemble via end-to-end binding but lack secondary lateral interactions lead to 1D aggregation in the solid state and thus a lack of strength in the axis of the material perpendicular to the orientation of the hydrogen bonding system.

As part of this study, three relatively inexpensive residues based on a central aliphatic tertiary amine motif were selected as the polymer end groups. The tertiary amine element acted as a hydrogen bonding acceptor, whereas the nonplanar geometry of this unit was predicted to hinder crystallization of the end groups. Two of the substituents on the tertiary amine were butyl groups (without hydrogen bonding capability), part of a cyclic ether (morpholine, which may be considered a hydrogen bonding acceptor), or two alcohol moieties (which can act as hydrogen bond acceptors and donors). Lastly, the end group was introduced to the isocyanate termini of the prepolymer either via an alcohol (Figure 1, 1–3) or amine functionality (Figure 1, 4–6) to afford the corresponding urethane or urea moieties, respectively. We have previously shown that the addition of these end groups (1–6) to methylene diphenyl diisocyanate (MDI) leads to polymeric-like materials.<sup>17</sup> These materials possess an irregular hydrogen-bonded array as a consequence of the conformational flexibility of the end groups disfavoring supramolecular linear chain extension, delivering the 3D morphology that generates mechanical robust materials.

Prior to the study of the self-assembling polymeric systems, model compounds featuring the hydrogen bonding end groups (1–6) were synthesized<sup>17</sup> to verify that their hydrogen bonding properties met the design criteria (7–12 in Table 1). Each model compound contained one of the end groups in addition to an aliphatic group that was designed to replicate the polymer chain.<sup>20</sup> In some cases, it was necessary to use a branched aliphatic residue (2-ethyl hexanol) to aid the solubility of the final product. It was possible to ascertain the self-associative

**Scheme 1.** Synthesis and Structures of Supramolecular Self-Assembling Polymers 15–20

binding constants of these model compounds (7–12) in solution (CDCl<sub>3</sub>, 25 °C). This was accomplished by measuring the change in position of the key NH proton resonances on the urethane (and/or the urea when present) with respect to concentration.<sup>17</sup> The binding constants for the six model compounds are reported in Table 1. (See the Supporting Information.)

As predicted, the binding constants for the model compounds correlated with increasing hydrogen bonding potential of the end groups in the order dibutyl < morpholine < diol within the series of compounds that contained either two urethane moieties (7, 8, and 9) or a combination of a urea and a urethane functionality (10, 11, and 12). In each case, the binding constant for the model compound that contained both urea and urethane groups was higher than that for the analogous model compound that contained two urethane groups. In all cases, the binding constant was low (between 1 and 45 M<sup>−1</sup>), far below that needed to produce an appreciable DP in dilute solution.<sup>8</sup>

With this data in hand, attention turned to the synthesis of the polymeric systems (15–20), which would be modified to contain the end groups 1–6. The synthesis of these supramolecular polymers was achieved by the addition of 2 equiv of the alcohol- or amine-functionalized end groups (1–6) to a prepolymer (14) synthesized by the addition of MDI to poly(ethylene-co-butylene) diol (13, [P(E-co-B)]) (NCO/OH 2:1), according to our previously established methodology<sup>18</sup> (Scheme 1) to deliver a prepolymer with a predicted molecular weight of 12 kDa. (See the Supporting Information.) We predicted that the nonpolar nature of P(E-co-B) would induce phase separation from the polar, hydrogen bonding end groups and aid the delivery of the desired supramolecular hydrogen-bonded elastomers.

As a consequence of the high reactivity of the prepolymer isocyanate end groups, the molecular weight of 14 could not be directly measured. However, the averaged  $M_n$  value of the polymers 15–20 was 14 kDa, as determined by GPC analysis, which was comparable to the targeted molecular weight of 12 kDa.



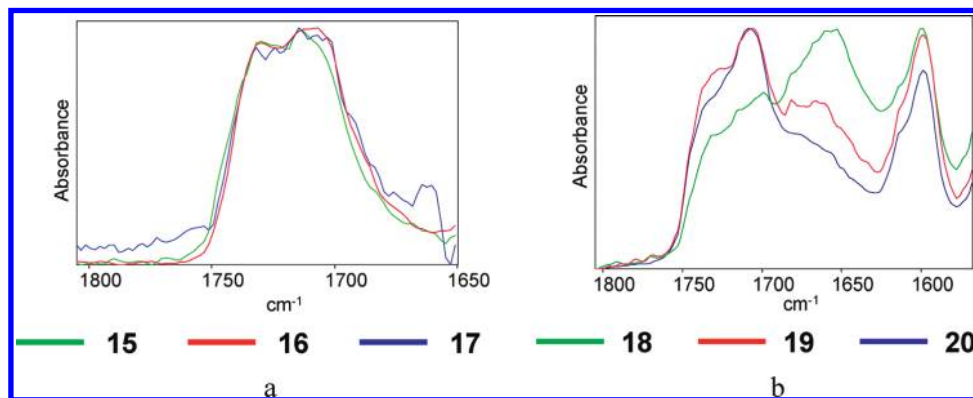


Figure 2. (a) Partial FTIR spectra for polymers 15–17 and (b) polymers 18–20.

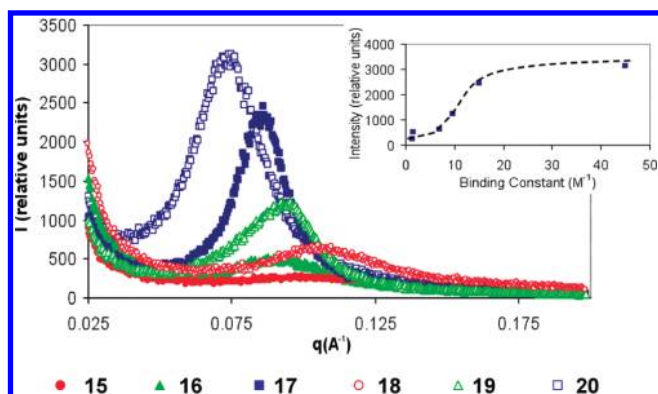


Figure 3. SAXS analysis of polymers 15–20 at 25 °C. Insert: plot of peak scattering intensity versus binding constant.

Each of the supramolecular polymers **15** to **20** was isolated as a rubberlike material that was soluble in organic solvents such as chloroform and THF. In contrast with the prepolymer **14**, a sticky viscous material under ambient temperature, the polymers (**15** to **20**) could be solution cast to form optically transparent, self-supporting elastomeric films, thus demonstrating the effect that the end groups have on the physical properties of the P(E-co-B) prepolymer **14**. It should be noted that as a consequence of the closely related composition of the polymers (**15**–**20**) each contained essentially the same proportion of hard block segments ( $11 \pm 0.4\%$ ). Therefore, differences in the morphology and mechanical performance within this series of polymers must be related to the small structural changes within the end group of each polymer.

To confirm that these polymers met the design criteria (*vide supra*), each of the samples was analyzed by solid-state FTIR and differential scanning calorimetry (DSC). The FTIR spectra for the polymers containing end groups appended to the prepolymer (**14**) via a urethane linkage (**15**–**17**) or urea linkages (**18**–**20**) are shown in Figure 2a,b, respectively. The FTIR spectra for urethane-terminated polymers **15**–**17** all exhibited strong absorbances for both the free ( $1730\text{ cm}^{-1}$ ) and hydrogen-bonded ( $1710\text{ cm}^{-1}$ ) urethane groups.<sup>21</sup> These spectroscopic data suggest that a proportion of the urethane groups are distributed throughout the soft segment rather than constrained within densely hydrogen-bonded hard segments.<sup>16</sup> In addition, IR spectroscopic analysis of polymers **18**–**20** (which contain both urethane and urea moieties) revealed absorbance bands corresponding to both free and hydrogen-bonded urethane groups ( $1730$  and  $1710\text{ cm}^{-1}$ , respectively) as well as intense bands indicative of disordered urea stacking ( $1660$ – $1680\text{ cm}^{-1}$ ). Absorbances consistent with ordered urea domains (ca.  $1630\text{ cm}^{-1}$ ) were, in contrast, relatively weak,

indicating that these materials did not feature significant crystalline domains, in line with our original design criteria.

Furthermore, the absence of crystallinity within all six polymers (**15**–**20**), was confirmed by DSC analysis. (See the Supporting Information.) Melting exotherms were not observed during either the heating or cooling cycles, thus demonstrating the desired amorphous morphology in all of these polymers. However, each thermogram featured a readily identifiable glass transition at ca.  $-60\text{ }^{\circ}\text{C}$ , typical of that expected for the P(E-co-B) soft segment.

To obtain a deeper understanding of the morphology of these materials, polymers **15**–**20** were analyzed by both wide-angle X-ray scattering (WAXS) and small-angle X-ray scattering (SAXS). Analysis of the WAXS scattering patterns confirmed the lack of crystallinity of the end groups but revealed the local packing of the self-assembled polymer network through the planar hydrogen bonds between the urethane or urea groups. All of the WAXS scattering patterns featured an isotropic halo at  $2\theta$ , which indicated a lattice spacing of  $4.7\text{ }\text{\AA}$  for the stacking of the urethane/urea moieties.<sup>22</sup> This lattice spacing was consistent regardless of the polymer end group under analysis.

Each of the polymers (**15**–**20**) exhibited a single Bragg peak in the SAXS profiles, suggesting a microphase-separated morphology on the  $5.9$ – $8.1\text{ nm}$  length scale (Figure 3). The phase separation is driven by the immiscibility of the hard, hydrogen bonding end groups within the soft, nonpolar central P(E-co-B) blocks. The intensity of the scattering signal increased with the type of end group in the order dibutyl < morpholine < diol. For each of these end groups, the urethane/urea-containing polymers (**18**–**20**) produced scattering signals with higher intensity when compared with the polymers (**15**–**17**) that possessed only urethane moieties. The relationship between the dilute solution binding constant for the end groups and the bulk peak scattering intensity is illustrated in Figure 3.

The intensity of the scattering signal is related to the degree of phase separation; therefore, increasing the binding constant increases the phase separation between the soft and hard sections. It can be seen for polymers **15**–**17**, which contain end groups with very low binding constants (ca.  $1$  to  $7\text{ M}^{-1}$ ), there is little increase in the absolute scattering signal ( $250$ – $600$  units). In contrast, further increase in binding constant of the end group from  $7$ – $15\text{ M}^{-1}$  (**17**–**19**) results in a dramatic increase in the scattering intensity from  $500$  to  $2500$  units. However, further tripling of the binding constant of the end group to  $45\text{ M}^{-1}$  (**20**) had a much smaller effect on the degree of phase separation with the scattering intensity only increasing to ca.  $3100$  units. These data suggest that there is a minimum binding constant necessary to produce appreciable phase separation, but in addition, there is a point at which maximum phase separation has been achieved, and a

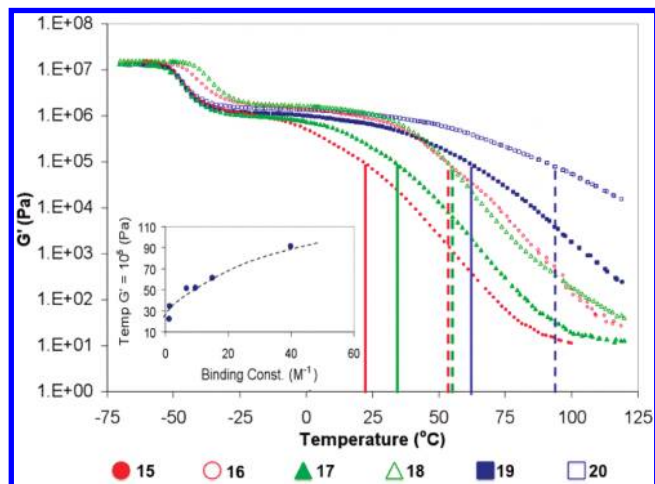


**Figure 4.** Variation of storage modulus with temperature for supramolecular polymers **15**–**20**. Insert: Plot of end group binding constant against the temperature at which the storage modulus for the respective polymers falls below  $10^5$  Pa.

further increase in the binding constant provides only limited changes to the polymer morphology.

Rheological analysis of the supramolecular polymers (**15**–**20**) was carried out on a parallel plate rheometer operating at a constant frequency of 10 Hz with a temperature ramp of 3 °C/min. Storage moduli were measured as a function of temperature over the range  $-75$  °C to at least 100 °C. All of the polymers appeared<sup>23</sup> to exhibit a drop in storage modulus between  $-35$  and  $-60$  °C from ca.  $10^7$  to  $10^6$  Pa, consistent with a phase transition occurring in the soft P(E-co-B) segments of the blend (Figure 4). The storage modulus for each polymer remained constant at this plateau ( $\sim 10^6$  Pa) until it began to reduce significantly as the temperature was increased. The end of the plateau region occurs at a temperature between 0 and 50 °C, depending on the molecular structure of the material. This rheological profile is entirely consistent with a multiphase morphology and has been previously observed for a range of structurally diverse, segmented poly(urethanes) in the solid state.<sup>24,25</sup>

The effect of structure on the rheological profile is further evident from the relationship between end-group binding constant in dilute solution and the temperature at which storage modulus for each polymer in bulk deviates from the plateau region (Figure 4, insert) (as defined by the temperature at which the storage modulus drops below  $10^5$  Pa). Therefore, whereas the storage modulus of the polymers at low temperatures (i.e., below 0 °C) is independent of the nature of the end group, the temperature at which the storage modulus deviates from the plateau region is directly related to the binding constant.

The high thermal responsiveness of these polymers may be exemplified by studying the rheological response of the morpholine end-capped supramolecular polymer **19** ( $M_n = 11\,000$  g mol<sup>-1</sup>), which exhibits a reduction in storage modulus of five orders of magnitude from  $10^6$  Pa between 50 and 100 °C. The material is thus transformed from a tough rubberlike elastomer to a free-flowing liquid. This is different to classic high-molecular-weight phase-segmented poly(urethanes), which typically exhibit reductions in storage modulus of only three orders of magnitude to  $10^6$  Pa at far higher temperatures (150–200 °C).<sup>26</sup>

## Conclusions

Through careful design, we have synthesized six new thermoplastic elastomers that possess weakly hydrogen bonding end groups. Our studies have shown that a variation of physical

properties correlate systematically with the hydrogen bonding strength of the end group. Binding constants in dilute solution, bulk SAXS peak scattering intensity, and storage modulus above ambient temperature all increased when the end group was changed from dibutyl < morpholine < diol and when the polymers contained urea groups. All of the polymers exhibited microphase separation in the bulk, and both the morphology and rheology correlated with the binding constant of the end groups in the dilute solution. These results signify an important design principle in the advance of supramolecular polymeric materials. We hope to develop further the observations made for this system to provide a general, predictive model for de novo design of supramolecular polymer materials.

**Acknowledgment.** We would like to thank Henkel U.K. Limited (postgraduate studentships for P.J.W. and D.H.M.) and EPSRC (EP/D07434711, EP/G026203/1 – postdoctoral fellowships for B.W.G.) and the University of Reading for financial support of this research.

**Supporting Information Available:** Full synthetic procedures, characterization, and <sup>1</sup>H NMR binding studies for model compounds **7**, **8**, and **10**–**12**. Calculation to estimate the molecular weight of prepolymer **14**. Full synthetic procedures and characterization for polymers **16** and **18**–**20**. <sup>1</sup>H and <sup>13</sup>C NMR spectra and DSC thermograms for polymers **15**–**20**. This material is available free of charge via the Internet at <http://pubs.acs.org>.

## References and Notes

- (1) Brunsveld, L.; Folmer, B. J. B.; Meijer, E. W.; Sijbesma, R. P. *Chem. Rev.* **2001**, *101*, 4071–4097.
- (2) For recent reviews on the synthesis and properties of supramolecular polymers, see: (a) Ciferri, A. *Supramolecular Polymers*; Marcel Dekker: New York, 2000. (b) Schmuck, C.; Wienand, W. *Angew. Chem., Int. Ed.* **2001**, *40*, 4363–4369. (c) Ciferri, A. *Macromol. Rapid Commun.* **2002**, *23*, 511–529. (d) Sivakova, S.; Rowan, S. J. *Chem. Soc. Rev.* **2005**, *34*, 9–21. (e) South, C. R.; Burd, C.; Weck, M. *Acc. Chem. Res.* **2007**, *40*, 63–74. (f) Fox, J. D.; Rowan, S. J. *Macromolecules* **2009**, *42*, 6823–6835.
- (3) Sijbesma, R. P.; Beijer, F. H.; Brunsveld, L.; Folmer, B. J. B.; Hirschberg, J. H. K. K.; Langer, R. F. M.; Lowe, J. K. L.; Meijer, E. W. *Science* **1997**, *278*, 1601–1604.
- (4) For reviews assessing recent developments in hydrogen bonded supramolecular polymers, see: (a) ten Cate, A. T.; Sijbesma, R. P. *Macromol. Rapid Commun.* **2002**, *23*, 1094–1112. (b) Shimizu, L. S. *Polym. Int.* **2007**, *56*, 444–452. (c) Wilson, A. J. *Soft Matter* **2007**, *3*, 409–425.
- (5) For examples of supramolecular polymer arrays formed via metal–ligand interactions, see: (a) Michelson, U.; Hunter, C. A. *Angew. Chem., Int. Ed.* **2000**, *39*, 764–767. (b) Beck, J. B.; Rowan, S. J. *J. Am. Chem. Soc.* **2003**, *125*, 13922–13923. (c) Zhao, Y. Q.; Beck, J. B.; Rowan, S. J.; Jamieson, A. M. *Macromolecules* **2004**, *37*, 3529–3531. (d) Hofmeier, H.; Schubert, U. S. *Chem. Soc. Rev.* **2004**, *33*, 373–399.
- (6) (a) Ashton, P. R.; Claessens, C. G.; Hayes, W.; Menzer, S.; Stoddart, J. F.; White, A. J. P.; Williams, D. J. *Angew. Chem., Int. Ed.* **1995**, *34*, 1862–1865. (b) Asakawa, M.; Ashton, P. R.; Brown, G. R.; Hayes, W.; Menzer, S.; Stoddart, J. F.; White, A. J. P.; Williams, D. J. *Adv. Mater.* **1996**, *8*, 37–41. (c) Asakawa, M.; Ashton, P. R.; Brown, G. R.; Hayes, W.; Janssen, H. M.; Meijer, E. W.; Menzer, S.; Pasini, D.; Stoddart, J. F.; White, A. J. P.; Williams, D. J. *J. Am. Chem. Soc.* **1998**, *120*, 920–932. (d) Burattini, S.; Colquhoun, H. M.; Greenland, B. W.; Hayes, W. *Faraday Discuss.* **2009**, *143*, 247–264. (e) Burattini, S.; Colquhoun, H. M.; Fox, J.; Friedmann, D.; Greenland, B. W.; Harris, P. J. F.; Hayes, W.; Mackay, M. E.; Rowan, S. J. *Chem. Commun.* **2009**, 6717–6719.
- (7) Ciferri, A. *Growth of Supramolecular Structures: Supramolecular Polymers*, 2nd Ed.; Ciferri, A. Ed.; CRC Press: Boca Raton, 2005.
- (8) (a) Ky Hirschberg, J. H. K.; Beijer, F. H.; van Aert, H. A.; Magusin, P. C. M. M.; Sijbesma, R. P.; Meijer, E. W. *Macromolecules* **1999**, *32*, 2696–2705. (b) Folmer, B. J. B.; Sijbesma, R. P.

- Kooijman, H.; Spek, A. L.; Meijer, E. W. *J. Am. Chem. Soc.* **1999**, *121*, 9001–9007. (c) Langer, R. F. M.; van Gurp, M.; Meijer, E. W. *J. Polym. Sci., Part A: Polym. Chem.* **1999**, *37*, 3657–3670. (d) Kautz, H.; van Beek, D. J. M.; Sijbesma, R. P.; Meijer, E. W. *Macromolecules* **2006**, *39*, 4265–4267.
- (9) (a) Park, T.; Zimmerman, S. C.; Nakashima, S. *J. Am. Chem. Soc.* **2005**, *127*, 6520–6521. (b) Park, T.; Todd, E. M.; Nakashima, S.; Zimmerman, S. C. *J. Am. Chem. Soc.* **2005**, *127*, 18133–18142. (c) Todd, E. M.; Quinn, J. R.; Zimmerman, S. C. *Isr. J. Chem.* **2005**, *45*, 381–389. (d) Park, T.; Mayer, M. F.; Nakashima, S.; Zimmerman, S. C. *Synlett* **2005**, 1435–1436.
- (10) St. Pourcain, C. B.; Griffin, A. C. *Macromolecules* **1995**, *28*, 4116–4121.
- (11) Lillya, C. P.; Baker, R. J.; Hütte, S.; Winter, H. H.; Lin, Y.-G.; Shi, J.; Dickinson, L. C.; Chien, J. C. W. *Macromolecules* **1992**, *25*, 2076–2080.
- (12) Yilgor, I.; Yilgor, E. *Polym. Rev.* **2007**, *47*, 487–510.
- (13) Muller, M.; Dardin, A.; Seidel, U.; Balsamo, V.; Ivan, B.; Spiess, H. W.; Stadler, R. *Macromolecules* **1996**, *29*, 2577–2583.
- (14) Colombani, O.; Barioz, C.; Bouteiller, L.; Chaneac, C.; Fomperie, L.; Lortie, F.; Montes, H. *Macromolecules* **2005**, *38*, 1752–1759.
- (15) (a) Arun, A.; Gaymans, R. J. *J. Appl. Polym. Sci.* **2009**, *122*, 2663–2668. (b) Öjelund, K.; Loontjens, T.; Steeman, P.; Palmans, A.; Maurer, F. *Macromol. Chem. Phys.* **2003**, *204*, 52–60. (c) Kuo, M.-C.; Jeng, R.-J.; Su, W.-C.; Dai, S. A. *Macromolecules* **2008**, *41*, 682–690.
- (16) Sivakova, S.; Bohnsack, D. A.; Mackay, M. E.; Suwanmala, P.; Rowan, S. J. *J. Am. Chem. Soc.* **2005**, *127*, 18202–18211.
- (17) (a) Woodward, P.; Clarke, A.; Greenland, B. W.; Hermida Merino, D.; Yates, L.; Slark, A. T.; Miravet, J. F.; Hayes, W. *Soft Matter* **2009**, *10*, 2000–2010. (b) Hayes, W.; Woodward, P. J.; Clarke, A.; Slark, A. T. Eur. Pat. EP792925, **2007**.
- (18) Woodward, P.; Hermida Merino, D.; Hamley, I. W.; Slark, A. T.; Hayes, W. *Aust. J. Chem.* **2009**, *62*, 790–793.
- (19) Botterhuis, N. E.; van Beek, D. J.; van Gemert, G. M. L.; Bosman, A. W.; Sijbesma, R. P. *J. Polym. Sci., Part A* **2008**, *46*, 3877–3885.
- (20) Söntjens, S. H. M.; Sijbesma, R. P.; van Genderen, M. H. P.; Meijer, E. W. *J. Am. Chem. Soc.* **2000**, *122*, 7487–7493.
- (21) Ning, L.; De-Ning, W.; Sheng-Kang, Y. *Polymer* **1996**, *37*, 3045–3047.
- (22) Kaushiva, B. D.; Wilkes, G. L. *J. Appl. Polym. Sci.* **2000**, *77*, 202–216.
- (23) It should be noted that the actual stiffness in the low-temperature region (below  $-50\text{ }^{\circ}\text{C}$ ) is likely to be higher than  $10^7\text{ Pa}$  because this is the upper limit of the modulus that can be measured using this instrument owing to the diameter of the plates used.
- (24) Sheth, J. P.; Klinedinst, D. B.; Wilkes, G. L.; Yilgor, I.; Yilgor, E. *Polymer* **2005**, *46*, 7317–7322.
- (25) (a) Versteegen, R. M.; Kleppinger, R.; Sijbesma, R. P.; Meier, E. W. *Macromolecules* **2006**, *39*, 772–783. (b) O'Sickey, M. J.; Lawrey, B. D.; Wilkes, G. L. *Polymer* **2002**, *43*, 7399–7408. (c) O'Sickey, M. J.; Lawrey, B. D.; Wilkes, G. L. *J. Appl. Polym. Sci.* **2003**, *89*, 3520–3529.
- (26) Pukánszky, B. Jr.; Bagdi, K.; Tóvölgyi, Z.; Varga, J.; Botz, L.; Hudak, S.; Dóczy, T.; Pukánszky, B. *Eur. Polym. J.* **2008**, *44*, 2431–2438.